Competition between unimolecular C–Br–bond fission and Br2 elimination in vibrationally highly excited CF2Br2

B. Abel, H. Hippler, N. Lange, J. Schuppe, and J. Troe

Citation: The Journal of Chemical Physics **101**, 9681 (1994); doi: 10.1063/1.467933
View online: http://dx.doi.org/10.1063/1.467933
View Table of Contents: http://scitation.aip.org/content/aip/journal/jcp/101/11?ver=pdfcov
Published by the AIP Publishing

Competition between unimolecular C–Br–bond fission and Br_2 elimination in vibrationally highly excited CF_2Br_2

B. Abel, H. Hippler,[a] N. Lange, J. Schuppe, and J. Troe
Institut für Physikalische Chemie der Universität Göttingen, Tammannstr. 6, D-37077 Göttingen, Germany

(Received 7 June 1994; accepted 17 August 1994)

The competition between C–Br–bond fission and three-center elimination of molecular bromine (Br_2) in highly excited CF_2Br_2 molecules has been studied under collision-free conditions. Transient resonantly enhanced multiphoton ionization (REMPI) was used to monitor $Br(^2P_{1/2})$ and $Br(^2P_{3/2})$ formation during and after infrared (IR) multiphoton excitation of CF_2Br_2; time-resolved laser-induced fluorescence (LIF) spectroscopy was employed for the detection of transient CF_2 after Br_2 elimination. Direct time-resolved measurements of the sum of afterpulse reaction rates, absolute product yields for the CF_2 and $Br(^2P_{3/2})$ channels as well as absorbed energies per excitation pulse were used to characterize parts of the vibrational energy distribution $P(E)$ established after IR multiphoton excitation and to determine rate coefficients and branching ratios for the elimination and dissociation reaction as a function of the average internal energy $\langle E \rangle$. The existence of both channels, the dissociation and the elimination channel, has been confirmed. A comparison of the experimental data with statistical adiabatic channel model calculations (SACM) enabled us to determine the threshold energies $E_0(J=0)$ for the unimolecular Br_2 elimination [$E_0(J=0)=19\ 070\pm500\ cm^{-1}$] and the C–Br bond fission [$E_0(J=0)=20\ 700\pm500\ cm^{-1}$], the two possible pathways of the reaction. © *1994 American Institute of Physics.*

I. INTRODUCTION

Time-resolved measurements of reaction rates, the identification of reaction products, and, in the case of competing channels, the determination of their relative yields is of fundamental interest in the understanding of unimolecular reactions.[1,2] Under thermal conditions, these quantities are not always easy to measure. The task becomes particularly difficult if branching ratios of competing channels are temperature- or pressure-dependent or if channel switching occurs.[3,4] In this situation nonthermal excitation techniques and methods for *in situ* identification of dissociation fragments, as well as measurements of selected rate coefficients and relative yields under collision-free conditions become desirable. In the present work we used IR multiphoton excitation for this purpose employing selective probing of reactants and products by time-resolved LIF or REMPI spectroscopy. We studied the CF_2Br_2 molecule as a model system for the competition of two reaction channels in a medium sized molecule.[3,4] In addition to this basic interest, CF_2Br_2 belongs to the group of brominated compounds which play an important role in atmospheric chemistry.[5–7]

A number of investigations have been reported on the photodissociation of this molecule using various excitation sources.[8–27] As shown in several publications,[8–24] vibrationally highly excited CF_2Br_2 molecules can conveniently be prepared by IR multiphoton excitation near 10 μm. The reaction of this molecule under multiphoton dissociation conditions was of interest in isotope separation experiments,[8] in addition to product analysis studies of the energetics and mechanism[8–19,23,24] of the process.

Basically, two different reaction channels with small differences in their threshold energies compete in the dissociation of CF_2Br_2 in its electronic ground state, the molecular elimination

$$CF_2Br_2 \xrightarrow{k_{el}} CF_2 + Br_2 \tag{1}$$

and the C–Br–bond fission

$$CF_2Br_2 \xrightarrow{k_{fis}} CF_2Br + Br(^2P_{3/2}). \tag{2}$$

Direct evidence for the presence of Br atoms,[11–13,19] CF_2 radicals,[9,17,18] Br_2 molecules,[17,18] and CF_2Br[23] radicals in CF_2Br_2 IR multiphoton decomposition experiments was obtained. The competition between the reaction channels is governed by the energy and angular momentum dependence of the individual specific rate constants $k(E,J)$. The rate constants $k(E,J)$ for the bond fission and elimination pathways and their dependence on the energy E and angular momentum J are quite different, due to the different nature of the corresponding "loose" and "tight" transition states. A theoretical treatment can be made with SACM/RRKM-type calculations, such as shown for the H_2CO and the toluene molecules.[3,4]

The two-channel character of the decomposition of vibrationally excited CF_2Br_2 became apparent in previous IR multiphoton excitation studies. In these experiments[8–19,23,24] TEA CO_2 laser pulses around 1078 cm^{-1} (9R22,9R24) were employed. In early experiments, Stephenson and King identified the elimination of Br_2 to be the primary channel[17,18] using laser-induced fluorescence (LIF) spectroscopy of Br_2 and CF_2. Subsequently, Sudbo *et al.*[12,13] showed in their molecular beam experiments that bromine atom elimination was the major channel. Later, Morrison *et al.*[9] confirmed the formation of CF_2 in the primary photodissociation of CF_2Br_2. They employed a product scavenging technique in combina-

[a]Institut für Physikalische Chemie und Elektrochemie, Universität Karlsruhe, Kaiserstr. 12, D-76199 Karlsruhe, Germany.

tion with gas chromatography to determine total and relative dissociation yields. Mittal *et al.*[23] used UV absorption spectroscopy and gas chromatography for the detection of CF_2Br and the identification of reaction products long after IR multiphoton excitation.

Measurements of final product yields have certainly provided considerable insight into the mechanism of CF_2Br_2 dissociation, especially after IR multiphoton excitation, although there is still some ambiguity about the existence of the elimination channel.[2,3] However, time-resolved measurements of reaction rates, *in situ* determinations of branching ratios, and detailed characterizations of excited state populations provide a more quantitative picture, in particular for the partly estimated threshold energies for the competing channels.

Because of the advantages of time-resolved measurements, we combined IR multiphoton excitation of CF_2Br_2 with transient REMPI and LIF detection of $Br(^2P_{3/2})$ and CF_2. With sensitive techniques the formation of dissociation products from different channels could be monitored *in situ* under low pressure conditions. Populations of vibrationally highly excited molecules were also probed similar to the technique described in Refs. 20 and 21. Although $CF_2Br_2^*$ molecules have only a weak absorption in the visible, they can be electronically excited and photolyzed. The photolysis fragment $Br(^2P_{1/2})$ can then easily be probed by REMPI spectroscopy, being a sensitive measure for excited state populations below and above the reaction threshold.[20,21] Once the vibrational energy distribution of vibrationally highly excited CF_2Br_2 molecules is characterized for given absorbed energies, absolute reaction yields, rate coefficients, and branching ratios, the unimolecular dissociation and the elimination channels, can be determined as a function of the internal energy $\langle E \rangle$. The time-resolved experiments provide a much clearer picture about the competition between different reaction channels in excited CF_2Br_2 than this was available before. The analysis of the experimental data by statistical adiabatic channel calculations[3,4,31–33] enabled us to improve estimates of the threshold energies E_0 for the elimination and the bond fission channels.

II. EXPERIMENTAL TECHNIQUE

Our experimental setup has partially been described in two recent publications.[20,21] Only the applied modifications will be given in detail here. Briefly, CF_2Br_2 molecules have been irradiated with well-defined short pulses (60–80 ns FWHM) from a TEA CO_2 laser oscillator/amplifier system such as described in Ref. 20. The oscillator operated at low N_2 pressures and was equipped with an intracavity cell filled with 4 mbar CF_3Br as a saturable absorber to avoid complications from long afterpulses. Unless noted otherwise, the CO_2 laser oscillator has been set to the 9R22 line at 1078.58 cm^{-1} which coincides with the symmetric C–F stretch transition of CF_2Br_2 in the IR.[54] Usually single mode pulses with nearly Gaussian time and spatial profiles, with variable pulse intensities and fluences between 0.3 and 3 $J\,cm^{-2}$/pulse, were employed in the experiments. CF_2Br_2 was obtained from Aldrich with a stated purity of 99%. It was degassed by several freeze–thaw–pump cycles prior to use. CF_2Br_2 was irradiated in two low pressure cells at pressures between 5 and 20 μbar. A slow steady flow in the cells avoided the accumulation of reaction products.

The decomposition of excited CF_2Br_2 molecules under collision-free conditions was followed by time-resolved LIF and REMPI spectroscopy. In the case of REMPI detection, multiphoton ionization of $Br(^2P_{1/2})$ and $Br(^2P_{3/2})$ bromine atoms was achieved by pulses from a Lambda Physik laser system.[20,21] Details of the REMPI detection cell and the pump–probe geometry have already been described earlier in Refs. 20 and 21.

In LIF experiments, where the reaction product CF_2 was sensitively and selectively probed by laser-induced fluorescence in the $A \leftarrow X$ system, a different cell has been employed. The stainless-steel cell was equipped with two tubes (brewster angle windows/"Wood horn" extensions) which contained light baffles to reduce scattered light from the pump and probe pulses. The approximately collinear (within 2°–3°) counterpropagating CO_2 laser pulse and the pulse from the dye laser (both unfocused) were overlapped in the central region of the cell. Vibrationally excited CF_2Br_2 molecules were prepared by IR multiphoton excitation at fluences between 0.4 and 3 J/cm^2. The excimer pumped dye laser was operated with sulforhodamin B/DMSO dye and equipped with a BBO I crystal/autotracker system to provide tunable UV radiation between 250 and 270 nm. Typical pulse energies were in the range of 1–2 mJ/pulse. The LIF was collected perpendicular to the two laser beams with two 50 mm focal length lenses ($f/2$). After passing a Zeiss monochromator (Zeiss M4QIII), the light was detected with a photomultiplier tube (RCA 1P28 A). The multiplier output was amplified and processed with a gated boxcar integrator. Energies and intensities of the two laser pulses were recorded with two pyroelectric detectors. The ion/LIF signals were discriminated with respect to both laser energies. The time delay was measured with a Ge photon drag detector (Rofin 7441) and a photodiode using a time interval counter (SR 632). As in Ref. 20, varying the time delay, averaging (four to ten experiments per delay), and data recording was controlled by a personal computer.

Figure 1 summarizes our detection scheme for the products and the parent molecule in the decomposition of vibrationally highly excited CF_2Br_2 molecules after IR multiphoton excitation. CF_2Br_2 molecules from a thermal (300 K) sample were excited by multiphoton absorption (absorption of up to 21 photons through the C–F stretch vibration). Molecules at energies above the reaction thresholds E_{01} and E_{02} (Fig. 2) have the possibility to react via the bond fission or the elimination channel. In the present experiments we probed absolute concentrations of excited parent molecules [by REMPI of its $Br(^2P_{1/2})$ photofragment], the $Br(^2P_{3/2})$ and CF_2 fragments as well as Br_2 [detected as $Br(^2P_{3/2})$ and $Br(^2P_{1/2})$ under our conditions]. We did not try to probe CF_2Br in the present experiments. In the following, details of the various detection schemes will be described.

After infrared multiphoton excitation $CF_2Br_2^*$ is probed by photolysis, yielding $Br(^2P_{1/2})$, which can be detected within the same probe laser pulse by REMPI:

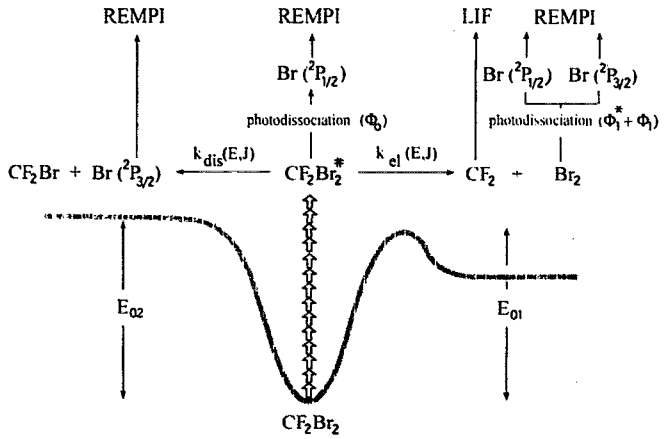

FIG. 1. Scheme for competing decompositions of vibrationally highly excited CF_2Br_2 molecules [the arrows indicate IR multiphoton excitation of CF_2Br_2 (⇑) and subsequent detection (↑) of the parent molecules by photodissociation/REMPI and of the reaction products of the two channels (Br_2,Br,CF_2) by LIF and REMPI; E_{01} and E_{02} are the threshold energies for the two competing reaction channels].

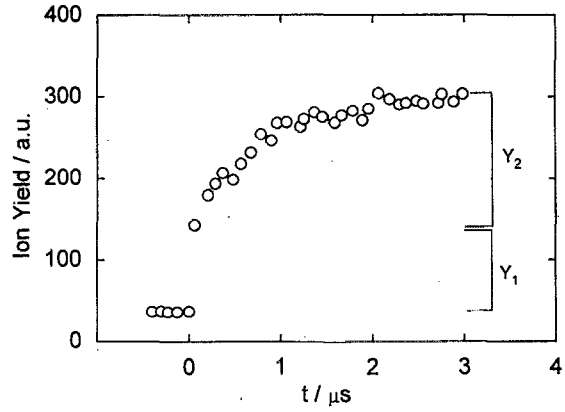

FIG. 3. Transient 3+2 REMPI signal of Br($^2P_{3/2}$), recorded at 462.02 nm during and after IR multiphoton excitation of CF_2Br_2 [excitation at 1078.58 cm^{-1} (R22), 1.10 J/cm^{-2}, 20 μbar]. The yields Y_1 and Y_2 are given in arbitrary units. They denote the overall formation of Br($^2P_{3/2}$) during and after the IR laser pulse, respectively, and lead to the fractions f_c^{dis}, f_c^{el}, f_b^{dis}, and f_b^{el} of Fig. 2 (see the text).

$$CF_2Br_2^* + h\nu \rightarrow Br(^2P_{1/2}) + CF_2Br. \quad (3)$$

A photolysis quantum yield of $\Phi_0[Br(^2P_{1/2})]=0.8-1$ was estimated by comparing time-resolved absolute Br($^2P_{3/2}$) and CF_2 yields for the two reaction channels and time-resolved Br($^2P_{1/2}$) traces (the absolute afterpulse yields for the loss of excited state molecules have been compared with absolute afterpulse product yields, therefore Φ_0 could be estimated from Y_2, Y_3, Y_5, and Y_6, which are shown in Figs. 3–5 and defined in Sec. III A, e.g., in the case of $\Phi_0=1$ the yield for the loss of excited state molecules calculated from Y_3 would be equal to the total reaction yield derived from Y_2). The sensitive detection of Br($^2P_{1/2}$) after the photolysis of $CF_2Br_2^*$ provided a quantitative estimate of $CF_2Br_2^*$ concentrations produced by IR multiphoton excitation (analogous to the experiments described in Refs. 20 and 21). The 3+2 REMPI transition of Br($^2P_{1/2}$) at 459.34 nm[28,29] was used for the detection. The 459 nm photolysis and the subsequent probe of excited Br atoms does, in principle, discriminate against different amounts of vibrational excitation of the parent $CF_2Br_2^*$ molecules, due to the energy dependence of its absorption coefficient.[20,21] Since the energy/temperature dependence of the absorption coefficient is not known very precisely, in this case, we could only distinguish between excited molecules and molecules which are not excited at all because the latter cannot be photolyzed effectively at 459 nm (because of the low absorption coefficient). The full spectrum of available Br($^2P_{3/2}$) and Br($^2P_{1/2}$) lines is easily recorded by introducing Br_2 into the

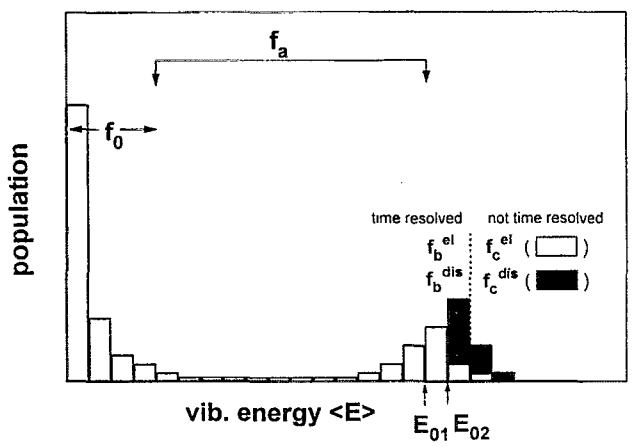

FIG. 2. Schematic bimodal energy distribution in IR multiphoton excitation of CF_2Br_2 (f_i=fractions of the population which could be distinguished in the present work, see the text).

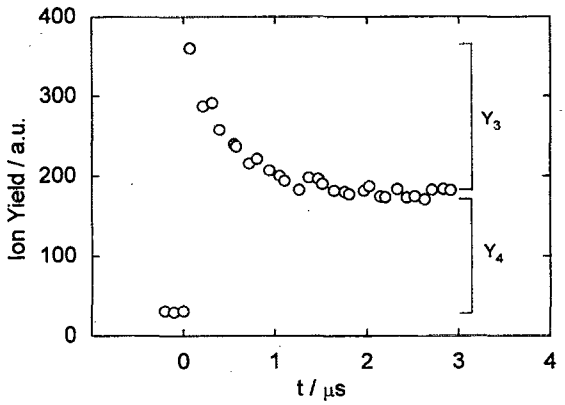

FIG. 4. Transient 3+2 REMPI signal of Br($^2P_{1/2}$), recorded at 459.34 nm and detecting excited $CF_2Br_2^*$ molecules via electronic excitation and photolysis during and after IR multiphoton excitation of CF_2Br_2 [excitation at 1078.58 cm^{-1} (R22), 1.4 J/cm^{-2}, 20 μbar of CF_2Br_2]. The yields Y_3 and Y_4 are given in arbitrary units. They lead to the fractions f_b^{dis}, f_b^{el}, f_c^{el}, and f_a of Fig. 2 (see the text).

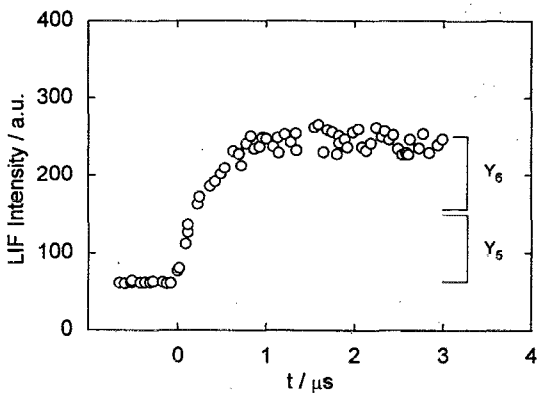

FIG. 5. Transient LIF signal of CF_2 [$A\ ^1B_1(020) \leftarrow X\ ^1A_1(000)$] recorded at an LIF excitation wavelength of 261.705 nm during and after IR multiphoton excitation [excitation at 1078.58 cm^{-1} (R22), 1.10 J/cm^{-2}, 10 μbar of CF_2Br_2]. The yields Y_5 and Y_6 are given in arbitrary units. They lead to the fractions f_c^{el} and f_b^{el} of Fig. 2 (see the text).

reaction cell. $Br(^2P_{3/2})$ atoms, which are the product from the IR multiphoton dissociation of CF_2Br_2 and from probe laser photolysis of Br_2:

$$Br_2 + h\nu \rightarrow Br(^2P_{1/2}) + Br(^2P_{3/2}) \tag{4}$$

can selectively and sensitively be detected by a 3+2 REMPI process at 462.02 nm.[28,29] The quantum yield for $Br(^2P_{3/2})$ and $Br(^2P_{1/2})$ in the photolysis of Br_2 has recently been measured in the employed wavelength region[42] $\{\Phi_1^*[Br(^2P_{1/2})]=0.63$ and $\Phi_1[Br(^2P_{3/2})]=1.37\}$. A small ionization background resulting from photodissociation of "cold" CF_2Br_2 molecules was subtracted on every other shot.

CF_2 concentrations from IR multiphoton dissociation of $CF_2Br_2^*$ were detected by (LIF) in the $A \leftarrow X$ band. The structure of the $A \leftarrow X$ band of CF_2 is well known.[24–26,38,39] In our experiments we tuned the probing dye laser to the maximum of the $CF_2\ A\ ^1B_1(020) \leftarrow CF_2\ X\ ^1A_1(000)$ band at 261.702 nm. Recording LIF excitation spectra of CF_2 after IR multiphoton dissociation in the range 250–270 nm, we were also able to determine product vibrational and rotational distributions of CF_2.

With the LIF and REMPI techniques described above, it was possible to measure transient concentrations of CF_2, $Br(^2P_{3/2})$, and $Br(^2P_{1/2})$ during and after IR multiphoton excitation. Using the quantum yields for the photodissociation of Br_2 and $CF_2Br_2^*$ in the wavelength region 455–465 nm, we were able to derive *total* reaction yields [from the $Br(^2P_{3/2})$ profiles] and absolute yields for the elimination channel alone. Due to the coupling of channels (1) and (2), time-resolved detection of $Br(^2P_{3/2})$ and CF_2 led to the sum $k_{el}+k_{dis}$. From the transient concentrations of $Br(^2P_{1/2})$ we were also able to get an estimate about total $CF_2Br_2^*$ concentrations above and below the reaction thresholds. The absolute yields of $Br(^2P_{3/2})$ and $Br(^2P_{1/2})$ and CF_2 could easily be calibrated by comparing signals from IR multiphoton experiments with the signals from well understood photolysis reactions of Br_2 (450 nm[42]) and C_2F_4 (193 nm[43]).

With our combined LIF/REMPI technique we have been able to probe different "parts" f_i of the rovibrational energy distribution, such as demonstrated recently.[20] The details of this characterization are illustrated in Fig. 2. In the following, the fraction of molecules, which are not excited at all, and of molecules, which are excited but remain below the reaction threshold, will be termed f_0 and f_a, respectively. The nomenclature is similar to that of Ref. 20. Depending on their internal energy E, the molecules above the reaction threshold are separated into fractions f_b and f_c. The decomposition of molecules close to the reaction threshold (fraction f_b) can be measured time resolved, whereas the reaction of molecules with more than 1000 cm^{-1} (e.g., one IR photon) of excess energy with respect to E_{02} (fraction f_c), proceeds within the excitation laser pulse, because of the strong energy and J dependence of the specific rate constants close to the reaction threshold. Due to the two reaction channels accessible in the decomposition of vibrationally excited CF_2Br_2, the fractions f_b and f_c have to be subdivided into f_b^{dis} and f_c^{dis} for the dissociation channel and f_b^{el} and f_b^{el} for the elimination channel, respectively. The fractions f_0, f_a, f_b^{dis}, f_c^{dis}, f_b^{el}, and f_c^{el} are characterized schematically in Fig. 2.

III. EXPERIMENTAL RESULTS AND DISCUSSION

A. Excited state yields

Figures 3 and 4 show typical transient REMPI signals of $Br(^2P_{3/2})$ and $Br(^2P_{1/2})$, recorded at 462.02 and 459.34 nm, respectively, during and after IR multiphoton excitation of CF_2Br_2 at 1078.58 cm^{-1} (9R22 line). The CF_2Br_2 pressure was kept at 10–20 μbar such that gas kinetic collisions over the time of the measurement could be neglected. The CO_2–laser fluence was 0.6–1.4 J/cm^2, the pulse width 60–80 ns (FWHM).

The initial step of the ion signal in Fig. 3 corresponds to an in-pulse formation of $Br(^2P_{3/2})$ (yield $Y_1 = f_c^{dis} + \Phi_1 f_c^{el}$) during the IR multiphoton dissociation of vibrationally excited CF_2Br_2 molecules (fraction f_c^{dis}) and the photolysis of Br_2 (a measure for f_c^{el}) by the probe pulse after the elimination reaction. The subsequent slower rise indicates a substantial after pulse reaction (yield at about 3 μs $Y_2 = f_b^{dis} + \Phi_1 f_b^{el}$). The fraction f_b corresponds to molecules whose internal energy $\langle E \rangle$ is close to the threshold energy E_0 whereas the molecules corresponding to fraction f_c (defined in Sec. II) contain more than one IR laser photon of excess energy and react within the excitation laser pulse. Information about f_b^{dis}, f_c^{dis}, f_b^{el}, and f_c^{el} can be obtained from Y_1 and Y_2 in Fig. 3, as well as information about the reaction rates of molecules close to the reaction thresholds. The reaction rates as well as reaction yields for the afterpulse reaction cannot be determined from this trace alone. Due to the coupled bond fission and elimination channels [see Eqs. (1) and (2)], the time constant of the slow rise in Fig. 3 corresponds to the sum $k_{el}+k_{dis}$. For the particular experiment of Fig. 3 in-pulse and afterpulse yields of $Br(^2P_{3/2})$ (Y_1 and Y_2) are close to each other. With increasing laser fluence and intensity, the relative yield for in-pulse reaction increases while the yield for the afterpulse reaction decreases. The amplitude of the signal at all times is a measure for the

combined reaction yield of both channels because $Br(^2P_{3/2})$ from the bond fission channel as well as $Br(^2P_{3/2})$ from photolysis of Br_2 by the elimination channel are detected in the experiment. The quantum yields and cross sections for quantitative photolysis under our experimental conditions were taken from Ref. 42.

While Fig. 3 documents the appearance of the dissociation product $Br(^2P_{3/2})$ and the elimination product Br_2, the $Br(^2P_{1/2})$ profile of Fig. 4 mainly corresponds to the disappearance of vibrationally highly excited $CF_2Br_2^*$ molecules, in analogy to our earlier experiments on CF_3I.[20,21] After photolysis of $CF_2Br_2^*$ molecules, the product $Br(^2P_{1/2})$ is a quantitative measure of the concentration of the energized parent molecules. Due to the interference from the Br_2 photolysis the evaluation of the experimental traces is slightly more complicated than in the CF_3I experiments of Refs. 20 and 21. We define the yields Y_3 and Y_4 at about 3 μs as indicated in Fig. 4 and given by $Y_3 = \Phi_0(f_b^{dis} + f_b^{el}) - \Phi_1^* f_b^{el}$ and $Y_4 = \Phi_0 f_a + \Phi_1^*(f_b^{el} + f_c^{el})$. The initial step in Fig. 4 corresponds to in-pulse excitation which in part is followed by fast in-pulse reaction [$Y_{t=0}$ can be defined as $Y_3 + Y_4 = \Phi_0(f_a + f_b^{dis} + f_b^{el}) + \Phi_1^* f_c^{el}$]. The signal at $t=0$ thus contains information about f_a, f_b^{dis}, f_b^{el}, and f_c^{el}. Molecules undergoing in-pulse dissociation (fraction f_c^{dis}) are not included here. The observed afterpulse decay can be attributed to the reaction of CF_2Br_2 molecules via the two possible channels forming $Br(^2P_{3/2})$ and CF_2Br and CF_2 and Br_2, respectively. This decay also contains afterpulse formation of $Br(^2P_{1/2})$ from the photolysis of Br_2 formed in the course of the elimination reaction. The afterpulse reaction again corresponds to molecules which are excited close to the reaction thresholds. The time profile of the slow decrease is consistent with the afterpulse signal in Fig. 3. The end signal of the decay provides a sensitive measure of molecules, which have been excited, but which did not have enough internal energy to react via the one or the other channel (fraction f_a); molecules which underwent elimination of $Br_2(f_b^{el} + f_c^{el})$ and finally led to $Br(^2P_{1/2})$ through the photolysis are also included. "Cold" CF_2Br cannot be photolyzed under our conditions[23] (it therefore does not affect the Br-REMPI probe). A vibrationally high excitation and a subsequent dissociation of this reaction product due to IR multiphoton excitation in the IR laser pulse is very unlikely under our low intensity/fluence excitation conditions.[12]

Figure 5 corresponds to an LIF signal of CF_2 recorded during (yield Y_5) and after (yield Y_6) IR multiphoton excitation. Analysing the CF_2 product state distributions after the reaction, no major vibrational excitation was detected. CF_2 generally was probed at 261.705 nm, the maximum of the $A\ ^1B_1(020) \leftarrow X\ ^1A_1(000)$ transition. Undispersed fluorescence at wavelengths above 280 nm was recorded. While the initial step in LIF intensity corresponds to CF_2 formation during the CO_2 laser pulse (yield $Y_5 = f_c^{el}$), the slower increase can be attributed to afterpulse formation of CF_2 (yield $Y_6 = f_b^{el}$). The transient signal corresponds to the elimination channel alone. The time dependence of Fig. 5 is again consistent with Figs. 3 and 4. The afterpulse rate of formation of CF_2 corresponds to molecules with small excess energy, the rate is again characterized by the sum $k_{dis}+k_{el}$. Because the

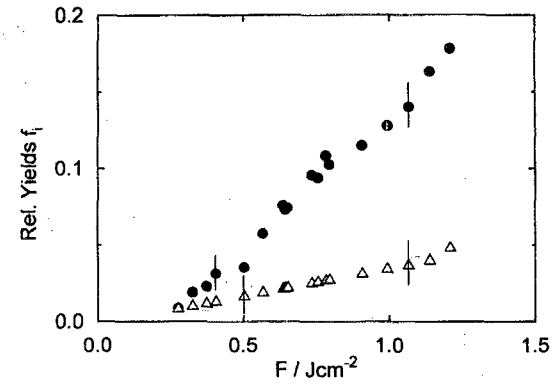

FIG. 6. Relative yields $f_a + f_b^{dis} + f_c^{dis} + f_b^{el} + f_c^{el}$ of *all excited state* molecules after IR multiphoton excitation of CF_2Br_2 (filled circles) and of excited state molecules f_a which are below the reactions thresholds and do not have enough energy to react via the one or other channel (open triangles) for different CO_2 laser fluences/intensities.

present experiments have been calibrated on an absolute basis, the relative yields described above could be converted into absolute excited state yields or absolute product yields. As described above, the $Br(^2P_{3/2})$ yields are a measure for the total reaction yields (see Fig. 2). LIF detection of the reaction product CF_2 on the other hand, provides absolute yields for the elimination channel alone. One, therefore, can separate the total yields into individual channel yields by subtraction. Together with the information on the fraction f_a from traces like in Fig. 4, individual absolute reaction yields for the two channels for the in-pulse (f_c^{dis} and f_c^{el}) and the afterpulse reaction (f_b^{dis}, f_b^{el}) and finally the yield of total excitation (f_a, $+ f_b^{dis} + f_c^{dis} + f_b^{el} + f_c^{el}$) are accessible. Figures 6 and 7 show the results of this procedure. Figure 6 gives the total excitation yields (filled circles) and the fraction f_a of molecules, which are excited but remain below the reaction thresholds (triangles), as a function of the excitation laser fluence. The ratio of the two quantities at each fluence is

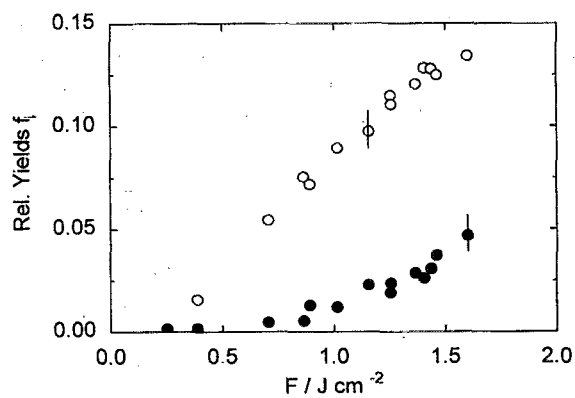

FIG. 7. Relative reaction yields $f_b^{el} + f_c^{el}$ for the elimination (filled circles) and $f_b^{dis} + f_c^{dis}$ for the dissociation channel (open circles) of CF_2Br_2 as a function of the laser fluence/intensity. The error bars for the calibrated yields are indicated.

almost constant, which suggests that the corresponding energy distribution is qualitatively not changing. Increasing the CO_2 laser fluence increases the population without changing the overall features of the energy distribution $P(E)$. Figure 7 represents the relative reaction yields for the bond fission channel (open circles) as a function of the CO_2 laser fluence, whereas the filled circles correspond to the elimination channel. For the two energetically close reaction channels in CF_2Br_2 the less advantageous bond fission to Br is favored. Krajnovich *et al.*,[19] Sudbo *et al.*,[12] and Mittal *et al.*[23] recently found that the yield of the dissociation channel amounts to about 90% of the total reaction yield. Morrison *et al.*[9] used Cl_2 as a scavenger in 40-fold excess over CF_2Br_2. Following the CO_2 laser irradiation, two products, CF_2BrCl and CF_2Cl_2, were detected which were interpreted as arising from the primary products CF_2Br and CF_2. In the intermediate fluence region, yields for the elimination reaction between 10% and 30% were found. At high fluences, little or no CF_2 was detected. The fact that CF_2 was observed at the smallest fluences seemed to support the conclusion that CF_2 was formed by the low-energy channel in the primary photodissociation of CF_2Br_2. Stephenson and King[17,18] detected the elimination channel via LIF of CF_2 and Br_2 such that they could not estimate the yield of the dissociation channel.

From Figs. 6 and 7 we find at low fluences (0.7 J/cm^2) a relative yield of about 90% for the bond fission channel, whereas a yield of 80%–75% at the higher fluences (1.2–1.3 J/cm^2) could be detected. At even higher fluences/intensities (>1.5 J/cm^2) we expect the yield for the bond fission reaction to increase again due to the increasing ratio k_{dis}/k_{el} (see Sec. III E). This behavior may be explained by the assumption that an excitation distribution driven barely above both reaction thresholds by a weak pulse will mostly yield CF_2Br because the rate constants for the elimination reaction are so small that almost every molecule will be stabilized before it reacts. Increasing the pumping intensity the maximum of the population distribution will be driven closer to the threshold for elimination, this would first increase the relative yield of the elimination channel (see Fig. 2). Because the rate of the bond fission channel increases faster with excitation energy than the rate of the elimination channel, a continued increase in pumping intensity will strongly refavor the bond fission reaction. In our case we obviously have not reached the high intensity limit where the bond fission is dominant and the elimination is almost suppressed. Moreover, our fluence/intensity range was not large enough to change the average energy of the excited molecules significantly (see Fig. 11). Comparing our yields and the observed fluence dependence results (Figs. 6 and 7) for the two reaction channels with the results of Morrison *et al.*,[9] Sudbo *et al.*,[12] and Mittal *et al.*[23] we find slightly different yields and a different fluence dependence. The data in Refs. 9 and 12 are in accord with a model showing a strong dependence of the yields and the average internal energies on the laser fluence. It is difficult to explain the deviations between our results and the results from Refs. 9, 12, and 23 because the experiments have been carried out under very different pressure and excitation conditions (fluences). We have used a transient dual detection of

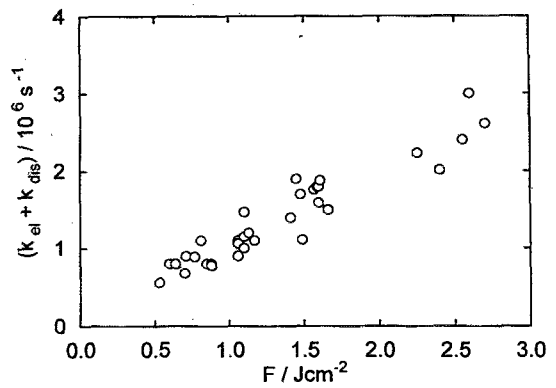

FIG. 8. Sum of rate constants $k_{el}+k_{dis}$ for the elimination and the dissociation channel of CF_2Br_2 as a function of the laser fluence/intensity (see the text).

both channels under near collision-free conditions (no secondary reactions, no collisional enhancement of the pumping process[21]) whereas in most of the earlier investigations indirect product detection (FTIR, gas chromatography) after a large number of shots has been employed. The molecular beam data from Ref. 12 cannot be easily compared with our results because the authors used much higher fluences/intensities. However, we believe that these data are still consistent with ours, assuming that they have reached the high fluence limit (monomodal energy distribution, $k_{dis} \gg k_{el}$).

B. Fluence/intensity dependence of the rate coefficients k_{el} and k_{dis}

From the transient Br($^2P_{3/2}$) and CF_2 profiles total decay rate constants $k_{el}+k_{dis}$ for excited CF_2Br_2 molecules were derived (see Fig. 8). With the branching ratios from Figs. 6 and 7 k_{el} and k_{dis} could be separated and studied as a function of the laser fluence. Figure 9 shows that k_{el} and k_{dis} increase with increasing laser fluence. The measured rate coefficients for the elimination and the dissociation channel, which include contributions from energy levels above (but

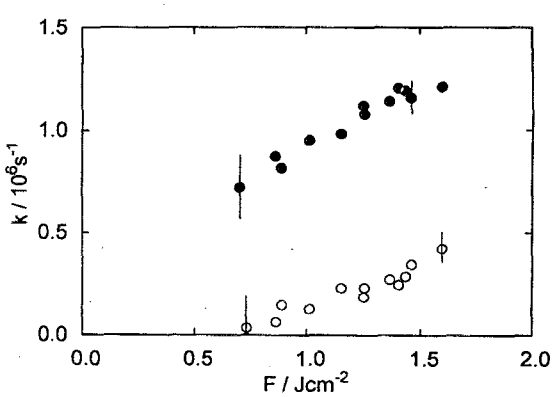

FIG. 9. Rate constants k_{el} for the elimination (open circles) and k_{dis} (filled circles) for the dissociation channel as a function of laser fluence/intensity.

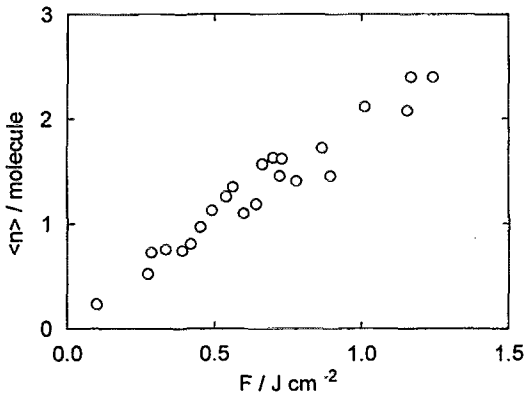

FIG. 10. Average number of IR photons [1078.58 $cm^{-1}(R22)$] absorbed per molecule as a function of laser fluence/intensity.

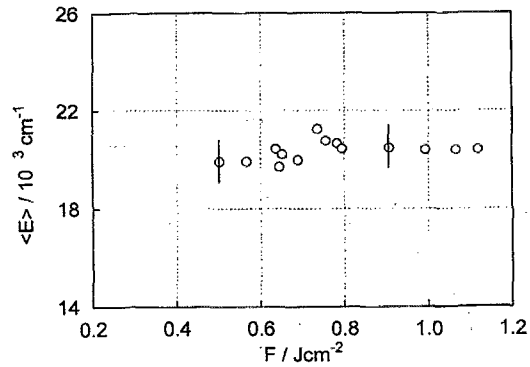

FIG. 11. Average internal energy of all excited molecules (filled circles in Fig. 6) as a function of laser fluence/intensity.

close to) the dissociation threshold were in the range between 1×10^5 and 1.5×10^6 s^{-1}. Our average rate coefficients for both channels after IR multiphoton excitation derived from time-resolved measurements can only be compared with an indirect estimate of the average rate constant for the bond fission from Ref. 23. In the fluence/intensity region at about 1 J/cm^2 they estimate an average $k_{dis}=1.8 \times 10^6$ s^{-1}.

C. Internal energy of the excited molecules

We also measured the absorbed energy of the molecules by subtracting the laser energy before and behind the cell containing the sample. The results are given in Fig. 10. As in other IR multiphoton excitation experiments, the average number of photons absorbed is quite low (2 for 1.0 J/cm^2), although a substantial fraction of molecules has been excited to energies above the reaction threshold. This experimental result can only be understood if one assumes a bimodal vibrational energy distribution.[20,21,53,54] Since we were able to determine the various fractions f_i of the vibrational energy distribution (see Sec. III A), we could estimate the average energy of the reacting molecules and of all excited molecules. The average energy of all excited molecules as a function of the laser fluence/intensity is displayed in Fig. 11. The internal energy of the excited molecules (high-energy part of the bimodal rovibrational energy distribution) seems not to depend on the fluence/intensity of the excitation laser in this particular fluence region, although the excited state yields, of course, change with changing excitation conditions. This is consistent with Fig. 6. We attribute this behavior to an enhanced pumping of those molecules, which are not excited efficiently at low energies/fluences, and we expect possible changes if the fluence/intensity of the excitation laser is further increased (see Refs. 9 and 12). The data in Fig. 11 and our conclusion that the internal energy of the molecules is hardly changed in the considered fluence region do not agree with the results of Refs. 9, 12, and 23. We tend to attribute the differences to different fluence and pressure ranges and/or to a different sensitivity of the applied techniques in the detection of excited state populations.

D. SACM calculations of specific rate constants

The elimination channel [Eq. (1)] is characterized by a tight, the C–Br–bond fission [Eq. (2)] by a loose transition state. Unfortunately, there is at present neither a reliable calculated potential energy surface nor an *ab initio* calculation available for a prediction of the corresponding activated complex parameters. There have been several RRKM calculations of the specific rate constants $k(E)$ for the elimination and the dissociation channels.[9,12,13] So far, these calculations do not provide a sufficiently detailed basis for an interpretation of experiments of the presented type. The hitherto neglected J dependence of the rate constants is of importance for both channels and has to be accounted for explicitly.

For this reason we calculated specific rate constants $k(E,J)$ of the two reaction channels using the statistical adiabatic channel model (SACM).[1,3,4,31–34] This model includes loose transition state as well as rigid activated complex RRKM theory. For $\alpha \rightarrow 0$ the rigid transition state RRKM theory and for $\alpha \rightarrow \infty$ the limit of phase space theory is approached. In between, it accounts for various kinds of anisotropy of the interaction potential between the dissociation fragments obeying angular momentum restrictions. Due to the lack of more detailed potential surface parameters, the simplified SACM version of Refs. 32 and 33 was employed using the parameters given in Appendix A. This calculation provided specific rate constants $k_{el}(E,J)$ and $k_{dis}(E,J)$ for the two channels such as given in Table I.

The results for the elimination channel correspond to J-dependent RRKM calculations.[2–4] For this channel, the contribution of the K rotor (in symmetric top notation) to the J-dependent vibrational density of states as well as to the J-dependent number of activated complex states has to be determined together with the proper J dependence of the threshold energy. One observes a strong increase of the threshold energy $E_0(J)$ with increasing J which, because of the very similar values of the rotational constants B and $B^{\#}$, is nearly equal to the rotational energy $BJ(J+1)$. The threshold rate constant $k[E_0(J)]$ drops markedly below the rate constants for $J=0$ and the curves for the specific rate constants $k(E,J>0)$ are essentially only shifted against the curve for $J=0$ by $BJ(J+1)$, due to an approximate com-

TABLE I. Specific rate constants $k(E,J)$ and threshold energies $E_0(J)$ for the bond fission and the elimination of CF_2Br_2.

	$k^{el}(E,J)(s^{-1})$		$k^{fis}(E,J)(s^{-1})$	
E (cm^{-1})	$J=0$	$J=100$	$J=0$	$J=100$
19 070	4.2×10^{3}			
20 070	5.9×10^{4}			
21 070	1.2×10^{6}	1.4×10^{4}	2.0×10^{6}	
22 070	7.9×10^{6}	4.2×10^{5}	9.1×10^{7}	6.9×10^{6}
23 070	3.0×10^{7}	5.0×10^{6}	5.5×10^{8}	2.4×10^{8}
24 070	8.7×10^{7}	2.0×10^{7}	2.2×10^{9}	1.8×10^{9}
25 070	2.0×10^{8}	5.9×10^{7}	5.3×10^{9}	5.2×10^{9}
26 070	4.1×10^{8}	1.4×10^{8}	1.2×10^{10}	1.2×10^{10}
27 070	7.4×10^{8}	3.2×10^{8}	2.1×10^{10}	2.1×10^{10}
28 070	1.2×10^{9}	5.8×10^{8}	4.2×10^{10}	4.2×10^{10}

J	$E_0^{fis}(J)(cm^{-1})$	$E_0^{el}(J)(cm^{-1})$
0	20 700	19 070
10	20 700	19 082
30	20 710	19 171
70	20 770	19 610
100	20 790	20 168
130	20 970	20 921
170	21 180	22 230
200	21 380	23 440

pensation of the rotational effects in $\rho(E,J)$ (density of states) and $W(E,J)$ (number of open channels or number of activated complex states).

The angular momentum and energy dependence of the specific rate constants of both channels is markedly different. Especially for the bond fission channel there is only a weak J dependence of the threshold energy and a steeper energy dependence. Also the J dependence of the $k(E,J)$ is quite different. It is, therefore, not surprising that the $k(E,J)$ as a function of E and J intersect and that "rotational channel switching" occurs at approximately $J\approx140$. These phenomena cause a complicated competition between the two channels at internal energies corresponding to the present excitation conditions.

One should also keep in mind that the specific rate constants could not be "calibrated" by comparison with thermal experiments (see Ref. 4). Therefore, the "looseness parameter" α and the threshold energies E_{01} and E_{02} were free parameters, adjusted to match the experimental data. Nevertheless, this modeling provided a complete and internally consistent set of specific rate constants, the prediction of a "rotational channel switching" and threshold energies for the two competing processes (Tables I and II). Table II also includes the limits within which the threshold energies could be varied to reproduce our results.

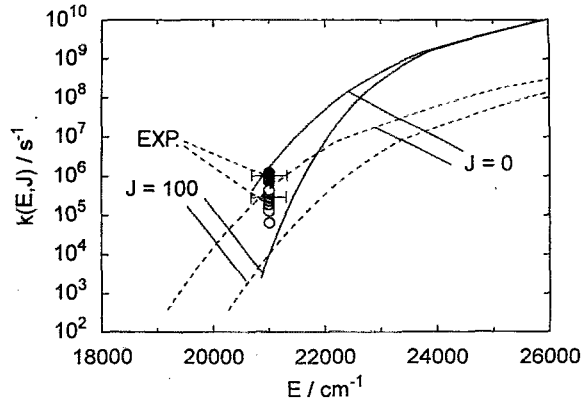

FIG. 12. Calculated specific rate constants $k(E,J)$ for the dissociation $CF_2Br_2\rightarrow CF_2Br+Br$ (bold lines) and the elimination $CF_2Br_2\rightarrow CF_2+Br_2$ (dashed lines) for $J=0$ and $J=100$. Also given are experimental rate constants k_{exp} (k_{el},k_{dis}) for the elimination and the bond fission channel as a function of the average internal energy $\langle E\rangle$ (EXP.: time-resolved data from this work; filled circles: bond fission, open circles: elimination).

E. Average reaction rate coefficients $k_{el}(\langle E\rangle)$ and $k_{dis}(\langle E\rangle)$

Since the yields of the excited molecules above the dissociation threshold and the average absorbed energies have been measured an average internal energy $\langle E\rangle$ of the reacting molecules above the threshold could be assigned. The result of this procedure, which lead to $k_{el}(\langle E\rangle)$ and $k_{dis}(\langle E\rangle)$ as a function of the average internal energy, is shown in Fig. 12 (open circles: elimination; filled circles: bond fission). As shown in Sec. III C, the average internal energy of the reacting molecules was not changed significantly under our experimental conditions although an increase in the afterpulse dissociation rate could be measured (Fig. 9). On an absolute energy scale, these variations are quite small. One might, nevertheless, ask why there is an increase in the afterpulse dissociation rate when, at the same time, there is no substantial increase in the average internal energy $\langle E\rangle$. There may be two explanations: First, under different excitation conditions one might pump and prepare different rovibrational states with approximately the same internal energy but different average angular momentum. Second, an enhanced pumping with increasing laser intensity of thermally "preexcited" molecules from the initial Boltzmann distribution, which are not pumped at low excitation energies/fluences, is certainly possible as well. Due to the complicated dependence of both, the elimination and the dissociation rate, on internal energy E and J and the intersection of the two

TABLE II. Threshold energies $E_0(J=0)$ for the elimination and dissociation reaction.

	Ref. 18	Ref. 23	Ref. 9	Ref. 35	Ref. 12	This work
$CF_2Br_2\rightarrow CF_2Br+Br$						
$E_0(J=0)$ (cm^{-1})	24 000	22 730	20 900	21 180	21 330	20 700 ± 500
$CF_2Br_2\rightarrow CF_2+Br_2$						
$E_0(J=0)$ (cm^{-1})	17 800	17 800	20 900	···	19 230	19 070 ± 500

$k(E,J)$ curves, it is still difficult to identify the reason for the variation of the afterpulse rate coefficients. Figure 12 includes SACM calculations for the elimination and the dissociation channel at $J=0$ and 100 (see Sec. III D and Table I). The experimental rate coefficients $k_{el}(\langle E\rangle)$ and $k_{dis}(\langle E\rangle)$ (EXP) at an average internal energy $\langle E\rangle$ from this work are consistent with the calculated specific rate constants for the two channels.

It turned out to be difficult to compare the measured and calculated rate coefficients with lifetimes from earlier (time-resolved) investigations because most of the reported lifetimes have been estimated from total yield measurements. Sudbo *et al.*[12] report an average rate constant of $1-2\times10^8$ s^{-1} for the bond fission channel (the elimination channel is almost suppressed) for CF_2Br_2 molecules with an average excess energy of 2450 cm^{-1}. Their estimate for the lifetime and the internal energy of excited molecules from RRKM calculations is in reasonable agreement with our calculated lifetimes in Fig. 12 and they are consistent with our measured data. Modeling their yield data Morrison *et al.*[9] indirectly extracted a slightly different functional form for the lifetimes of excited molecules for both channels as a function of internal energy. Their estimate of the internal energy of the reacting molecules has been based upon a modeling of the populations with a parametrized Master equation.

The small values of the specific rate constants (Fig. 12) for the elimination channel in the energy range, where only this reaction is possible, explains why the dissociation channel appears always to be the dominant channel. At energies below the threshold energy for the bond fission, the rate constants for the elimination are so small that the molecules are easily stabilized by collisions before they react. In our experiments, these molecules only contribute to the fraction f_a of molecules which are highly excited but do not have enough energy for reaction. At higher internal energies the dissociation channel becomes dominant because of its larger $k(E,J)$. The rate constants for the bond fission in this case become at least one order of magnitude larger than for the elimination channel.

F. Characterization of the vibrational energy distribution $P(E)$ after IR multiphoton excitation

With the excited state yields from Sec. III A and the measured absorbed energies various parts of the vibrational energy distribution $P(E)$ could be characterized. In principle, $P(E)$ corresponds to groups of states which are about 1000 cm^{-1} apart (one IR laser photon). Because of the initial rotational and vibrational Boltzmann distribution these groups are washed out. Our estimate of $P(E)$ follows the method of Refs. 20 and 21. Single states were not accessible because we only probed total yields f_i and not single states, such as done recently for CF_3I in a double resonance experiment.[53] We have not modeled the excitation process with a Master equation approach. Instead we decided to present the determined absolute yields f_i schematically in Fig. 2 and quantitatively in Table III. As in the case of CF_3I,[20,21,53,54] we find strong evidence for a bimodal distribution resulting from the IR multiphoton excitation process at low to moderate laser intensities/fluences. Clear indications for the presence of a bimodal distribution are (i) the small number of average absorbed photons (two photons on average at 1 J/cm^2) and (ii) the absolute yields $f_i(i=a,b,c)$. Molecules close to the threshold have an internal energy equal to ~19–20 IR photons for the reaction via the one or other channel. This can only be understood if a large fraction of the molecules (about 80%–90%) is not excited at all. Since the excited state yields have been measured (Sec. III A and Table III) it is easy to distinguish between a Boltzmann distribution and a bimodal energy distribution. The absolute yield of excited state CF_2Br_2 molecules was less than 20% at all applied excitation conditions.

TABLE III. Measured yields f_i of the vibrational energy distribution (according to Fig. 2) after IR multiphoton excitation at a typical intermediate fluence of 1 J cm^{-2} (estimated error ~20%–30% of the numbers in the table).

f_0	f_a	$f_b^{dis}+f_c^{dis}$	$f_b^{el}+f_c^{el}$	$\Sigma f_a+f_b+f_c$
85%	4%	9.5%	1.5%	<20%

IV. CONCLUSIONS

The direct and time-resolved measurements of the sum of afterpulse reaction rates, absolute yields for the CF_2 and $Br(^2P_{3/2})$ channels as well as absorbed energies per excitation pulse of this work could be used to characterize the vibrational energy distribution $P(E)$ after IR multiphoton excitation and to determine rate coefficients as well as branching ratios for the elimination and bond fission channel as a function of the average internal energy $\langle E\rangle$. The vibrational energy distribution again shows strong bimodal character, similar to vibrational distributions in CF_3I observed in our recent work.[20,21] The existence and the competition of both channels, the dissociation and the elimination channel, was confirmed, but the C–Br–bond fission is the dominant channel under our experimental conditions, although it is energetically less advantageous. A fit of the calculated specific rate constants $k(E,J)$ to the experimental data within certain limits could be used to estimate threshold energies $E_0(J=0)$ for the unimolecular elimination and the bond fission processes. In summary, we have shown that IR multiphoton excitation in combination with sensitive LIF/REMPI probe for the reaction products provides access to the investigation of vibrationally highly excited molecules with competing reaction channels.

ACKNOWLEDGMENTS

The authors had many stimulating discussions with M. Quack, G. Seyfang, and G. Hancock. Financial support from the "Deutsche Forschungsgemeinschaft" (SFB 357, B. A.'s DFG fellowship) is gratefully acknowledged.

APPENDIX: MOLECULAR PARAMETERS FOR SACM CALCULATIONS

CF_2Br_2: vibr. freq.: Refs. 50 and 51; rotational constants: 0.1087, 0.0366, 0.0032 [cm^{-1}][24]

CF_2Br: vibr. freq.: Refs. 47–49; rotational constants:

0.221 25, 0.1140, 0.034 22 [cm^{-1}][52]
CF_2: vibr. freq.: Refs. 44–46; rotational constants: 2.948 08, 0.390 73, 0.052 28 [cm^{-1}][18]
Br_2: vibr. freq.: Ref. 36; rotational constant: 0.080 92 [cm^{-1}][36]
Bond fission channel: $CF_2Br_2 \rightarrow CF_2Br+Br$ [$E_0(J=0)=20\,700\ cm^{-1}$]
Centrifugal parameters[32]: $a_1=0.106\ 22$, $a_2=0.004\ 56$
Ratio between "looseness parameter" α and morse parameter β is given by $\alpha/\beta=0.5$, $\beta=4.8\ Å^{-1}$
Elimination channel: $CF_2Br_2 \rightarrow CF_2B+Br_2$ [$E_0(J=0)=19\,070\ cm^{-1}$]
Centrifugal parameters[32]: $a_1=0.215\ 05$, $a_2=0.011\ 56$
$\alpha/\beta \rightarrow 0$, $\beta=3.4\ Å^{-1}$, $E_0(J>0) \cong E_0(J=0)+BJ(J+1)$.
The procedure for a correlation between disappearing/conserved oscillators and product oscillators/rotational degrees of freedom and a detailed description of the SACM model are given in Refs. 31–33.

[1] J. Troe, *Proceedings of the 22nd Symposium (International) on Combustion* (The Combustion Institute, Pittsburgh, 1988), p. 843.
[2] R. G. Gilbert and S. C. Smith, in *Theory of Unimolecular and Recombination Reactions* (Blackwell, Oxford, 1990); J. I. Steinfeld, J. S. Francisco, and W. L. Hase, in *Chemical Kinetics and Dynamics* (Prentice Hall, Englewood Cliffs, NJ, 1989).
[3] J. Troe, J. Chem. Phys. **88**, 4375 (1984).
[4] K. Luther, J. Troe, and K.-M. Weitzel, J. Phys. Chem. **94**, 6316 (1990).
[5] S. A. Penkett, B. M. R. Jones, M. J. Rycroft, and D. A. Simmons, Nature **318**, 550 (1985).
[6] L. T. Molina, M. J. Molina, and F. S. Rowland, J. Phys. Chem. **86**, 2672 (1982).
[7] Y. L. Yung, J. P. Pinto, R. T. Watson, and S. P. Sander, J. Atmos. Sci. **37**, 339 (1980).
[8] K. Sugia, P. Ma, Y. Ishikawa, and S. Arai, Appl. Phys. B **52**, 266 (1991).
[9] R. J. Morrison, R. F. Loring, R. L. Farley, and E. R. Grant, J. Chem. Phys. **75**, 148 (1981).
[10] C. D. Cantrell, in *Topics in Current Physics: Multiphoton Excitation and Dissociation of Polyatomic Molecules* (Springer, Berlin, 1986).
[11] V. N. Bagratashvili, V. S. Letokhov, A. A. Makarov, and E. A. Ryabov, in *Multiple Photon Infrared Laser Photophysics and Photochemistry* (Harwood, New York, 1985).
[12] A. S. Sudbo, P. A. Shulz, E. R. Grant, and Y. T. Lee, J. Chem. Phys. **70**, 912 (1979).
[13] A. S. Sudbo, P. A. Shulz, E. R. Grant, Y. R. Shen, and Y. T. Lee, J. Chem. Phys. **68**, 1306 (1978).
[14] J. C. Stephenson, S. E. Bialkowski, and D. S. King, J. Chem. Phys. **72**, 1161 (1980).
[15] D. Krajnovich, Z. Zhang, L. Butler, and Y. T. Lee, J. Chem. Phys. **88**, 4561 (1984).
[16] T. R. Gosnell, A. J. Taylor, and J. L. Lyman, J. Chem. Phys. **94**, 5949 (1991).
[17] D. S. King and J. C. Stephenson, J. Chem. Phys. **69**, 1485 (1978).
[18] D. S. King and J. C. Stephenson, Chem. Phys. Lett. **51**, 48 (1977).
[19] D. Kraijnovich, F. Huisken, Z. Zhang, Y. R. Shen, and Y. T. Lee, J. Chem. Phys. **77**, 5977 (1982).
[20] B. Abel, H. Hippler, and J. Troe, J. Chem. Phys. **96**, 8863 (1992).
[21] B. Abel, H. Hippler, and J. Troe, J. Chem. Phys. **96**, 8872 (1992).
[22] B. Abel, B. Herzog, H. Hippler, and J. Troe, J. Chem. Phys. **91**, 890 (1989).
[23] R. K. Vatsa, A. Kumar, P. D. Naik, K. V. S. Rama Rao, and J. P. Mittal, Chem. Phys. Lett. **207**, 75 (1993).
[24] D. S. King, P. K. Schenk, and J. C. Stephenson, J. Mol. Spectrosc. **78**, 981 (1979).
[25] G. Dornhöfer, W. Hack, and W. Langel, J. Phys. Chem. **87**, 3456 (1983).
[26] W. Hack and W. Langel, J. Photochem. **21**, 105 (1983).
[27] L. T. Molina, M. J. Molina, and F. S. Rowland, J. Phys. Chem. **87**, 2672 (1982).
[28] R. M. Robertson, D. M. Golden, and M. J. Rossi, J. Chem. Phys. **89**, 2925 (1988).
[29] *Handbook of Chemistry and Physics*, edited by R. C. Weast (Chemical Rubber, Boca Raton, 1987).
[30] *Atomic Energy Levels*, edited by C. B. Moore, NSRDS-NBS 35 (U.S. GPO, Washington, D.C., 1971), Vol. 2, p. 159.
[31] M. Quack and J. Troe, Ber. Bunsenges. Phys. Chem. **70**, 912 (1975).
[32] J. Troe, J. Chem. Phys. **79**, 6017 (1983).
[33] L. Brouwer, C. J. Cobos, J. Troe, H. R. Dübal, and F. Crim, J. Chem. Phys. **86**, 6171 (1987).
[34] J. Troe, Phys. Chem. N. F. **161**, 209 (1989).
[35] *Thermochemical Properties of Individual Substances*, edited by L. V. Gurvich, I. V. Veyts, and C. B. Allock (Blackwell, Oxford, 1985), Vol. 2, p. 145.
[36] G. Herzberg, in *Molecular Spectra and Molecular Structure* (Krieger, Malabar, 1945, 1990), Vols. I, II, and III.
[37] K. P. Huber and G. Herzberg, in *Constants of Diatomic Molecules* (Van Nostrand Reinhold, New York, 1979).
[38] P. Venkatesvarlu, Can. J. Phys. **47**, 2525 (1969).
[39] P. Venkatesvarlu, Phys. Rev. **77**, 1049 (1950).
[40] C. W. Mathews, Can. J. Phys. **45**, 2355 (1967).
[41] S. A. Kudchadker and A. P. Kudchadker, J. Phys. Chem. Ref. Data **7**, 1290 (1978).
[42] H. K. Haugen, E. Weitz, and S. R. Leone, J. Chem. Phys. **83**, 3402 (1985).
[43] O. Suto and J. I. Steinfeld, Chem. Phys. Lett. **168**, 181 (1990).
[44] D. E. Mann and B. A. Thrush, J. Chem. Phys. **33**, 1 (1960).
[45] K. C. Kerr and G. C. Pimentell, Appl. Opt. **4**, 25 (1965).
[46] D. E. Milligan and M. E. Jacox, J. Chem. Phys. **48**, 1120 (1968).
[47] D. E. Milligan, D. E. Mann, M. E. Jacox, and R. A. Mitsch, J. Chem. Phys. **41**, 1199 (1964).
[48] M. E. Jacox, Chem. Phys. Lett. **53**, 192 (1978).
[49] T. R. Gosnell, A. J. Taylor, and J. Lyman, J. Chem. Phys. **94**, 5949 (1991).
[50] N. Rothman, P. F. Dever, D. Garcia, and E. Grunwald, J. Phys. Chem. **90**, 6464 (1986).
[51] A. Baldacci, A. Gambi, S. Giorgianni, and R. Visioni, Spectrochim. Acta Part A **43**, 455 (1987).
[52] Y. G. Papulov, L. V. Chulkova, and A. E. Stepanyan, Zh. Strukt. Khim. **13**, 956 (1972).
[53] G. v. d. Hoek, M. Jonker, D. H. Parker, C. A. Taatjes, and S. Stolte, Chem. Phys. Lett. **215**, 461 (1993).
[54] M. Quack, Infrared Phys. **29**, 441 (1989).